Impedance spectroscopy analysis of high-temperature phase transitions in sodium lithium niobate ceramics

2000 J. Phys.: Condens. Matter 12 7833

(http://iopscience.iop.org/0953-8984/12/35/317)

J. Phys.: Condens. Matter **12** (2000) 7833–7841. Printed in the UK PII: S0953-8984(00)14276-6

Impedance spectroscopy analysis of high-temperature phase transitions in sodium lithium niobate ceramics

M A L Nobre† and S Lanfredi‡§

† Departamento de Engenharia Metalúrgica e de Materiais, Escola Politécnica, Universidade de São Paulo, USP, 05508-900 São Paulo, SP, Brazil
‡ Instituto de Física de São Carlos, Universidade de São Paulo, USP, CP 369, 13560-970 São Carlos, SP, Brazil

E-mail: silvania@ifsc.sc.usp.br

Received 26 May 2000, in final form 18 July 2000

Abstract. An investigation was made of the sodium lithium niobate $Na_{0.85}Li_{0.15}NbO_3$ ceramics using permittivity properties. Permittivity measurements were carried out by impedance spectroscopy in a frequency range of 5 to 1.3×10^7 Hz and at temperatures ranging from 25 to 750 °C. The thermal stability of the dielectric behaviour was evaluated as a function of several thermal cycles. The permittivity response was found to depend on both the partial thermal cycle (heating or cooling cycle) and the number of cycles. Three phase transitions are proposed based on a maximum of permittivity response as a function of temperature. The dielectric behaviour and its relationship with the phase transition phenomenon are discussed.

1. Introduction

The solid solution of the $Na_{1-x}Li_xNbO_3$ system is a promising ferroelectric material with high frequency applications [1, 2]. Sodium lithium niobates have been reported in the literature as dielectric and piezoelectric materials [3]. In many applications, the high electromechanical coupling and significant mechanical quality offered by these materials have been the main criteria for an excellent material.

Many investigations of the physical properties of the perovskite type family of alkaline (Na, K) niobates have been reported. $NaNbO_3$, which is known to be antiferroelectric, belongs to the orthorhombic system at room temperature. X-ray diffraction and optical studies of this material have revealed seven phase transitions occurring between 163 K and 913 K [4]. Few studies, however, have been reported on the phase transitions of sodium lithium niobate.

The $Na_{1-x}Li_xNbO_3$ system has been found to be ferroelectric at room temperature for $x \geqslant 0.02$ [5, 6], while $NaNbO_3$ is ferroelectric only at values under 163 K.

Sadel *et al* [7] reported the existence of five phase transitions for $Na_{1-x}Li_xNbO_3$ systems between 163 K and 940 K, with the ferroelectric–paraelectric phase transition occurring at 640 K (T_c), and two ferroelectric and one paraelectric phases were observed for the same crystal under the Curie temperature, suggesting a transformation of first order. Increasing substitution of Na^+ for Li^+ in the $Na_{1-x}Li_xNbO_3$ system increases the latter's Curie temperature. At temperatures slightly above T_c in the paraelectric phase, the crystal returns to its original state. However, new domains are observed at 825 K. These domains disappear at 940 K,

§ Author to whom correspondence should be addressed.

0953-8984/00/357833+09$30.00

when the crystal becomes transformed into the cubic symmetry. This temperature is called the ferroelastic Curie temperature. Although several investigations on phase transitions have been made, few studies have been reported on the dielectric properties of the $Na_{1-x}Li_xNbO_3$ solid solution and its correlation with dielectric behaviour.

The ac analysis technique has been widely used to study the dielectric behaviour of amorphous and polycrystalline materials [8]. This technique, when applied to ceramics, allows the dielectric properties to be separated from those corresponding to the grain boundaries and their interface with electrodes.

This report presents the results of a study of the dielectric properties of sodium lithium niobate as a function of thermal cycles using impedance spectroscopy. A detailed investigation is presented of the dielectric behaviour of solid solution $Na_{0.85}Li_{0.15}NbO_3$ at high temperature. Emphasis is given to the phase transition process and its correlation with dielectric behaviour.

2. Experimental procedure

2.1. $Na_{0.85}Li_{0.15}NbO_3$ synthesis

Solid solution $Na_{0.85}Li_{0.15}NbO_3$ was synthesized by a chemical evaporation method. Lithium nitrate, sodium nitrate and a soluble niobium complex salt, $NH_4H_2[NbO(C_2O_4)_3]\dot{3}H_2O$ (Companhia Brasileira de Metalurgia e Mineração, CBMM, Brazil), were used as starting reagents.

An x-ray powder analysis showed only the diffraction lines of the orthorhombic phase of sodium niobate (JCPDS Card 33-1270). Further details of the synthesis procedure and apparatus are described in a previous paper [9, 10].

2.2. Compaction, sintering and electrical characterization procedure

Calcined solid solution powder was deagglomerated by dry milling in an agate mortar, followed by the addition of 2 wt% of polyvinyl butyral used as a binder. This mixture was pressed into disc form under 10 kPa uniaxial pressure followed by 100 MPa isostatic pressure. A pellet with 1.1 mm thickness and 12 mm diameter was characterized.

The pellet was slowly heated to 500 °C and left for 5 hours until the binder was completely burned out. Two hours' sintering was performed in air at 1150 °C. A 10 °C min^{-1} heating rate was employed, while the cooling rate was fixed by the thermal inertia of the furnace. A relative density of 97% of the theoretical density was reached.

Platinum electrodes were deposited on both faces of the sample by a platinum paste coating (Demetron 308A), which was then dried at 800 °C for 30 min.

The electrical measurements were performed in the frequency range of 5 Hz to 13 MHz, using a Hewlett–Packard HP 4192A impedance analyser controlled by a personal computer. A 500 mV ac signal was applied. The samples were placed in an appropriate sample holder with a two-electrode configuration and the ac measurements were taken in several stages from room temperature to 200 °C in 50 °C steps, from 230 °C to 400 °C in 20 °C steps and above 400 °C again in 50 °C steps. The temperature was held for 1 hour prior to each measurement. All the measurements were carried out in a dry air flow.

3. Results and discussion

3.1. Dielectric behaviour

The impedance relaxation can be ideally reported by Debye's expression, where the material is represented by a parallel circuit with a pure resistor (R) and an ideal capacitor (C):

$$Z^* = \frac{1}{1/R + \mathrm{j}\omega C} = \frac{R}{1 + \mathrm{j}\omega/\omega_0} \tag{1}$$

where $\omega_0 = 1/RC$ is the characteristic angle of the equivalent circuit and $\omega = 2\pi f$ is the angular frequency of the applied field.

When the Nyquist diagram plot is considered, the impedance measurements commonly show semicircular forms [11]. In high frequency regions, the impedance diagram typically corresponds to the bulk properties. The semicircle's diameter from the intercept with the real axis corresponds to the resistance contribution (R) of the bulk. At this point, the bulk capacitance, C_b, called the geometric capacitance, can be trivially derived from the relation $\omega = 1/RC_b$.

In most cases, however, a non-ideal situation is observed. The Debye expression (1) is modified by introduction of an n factor that is dependent on the temperature. This modification leads to the Cole–Cole equation [12]:

$$Z^* = \frac{R}{1 + (\mathrm{j}\omega/\omega_0)^{1-n}}. \tag{2}$$

This relation suggests that the centre of the semicircle obtained by plotting on the Nyquist diagram is located below the real axis. Moreover, when the sample displays high resistivity, normally at a low temperature, the Nyquist diagram is not completely defined. In this case, a typical fitting process [8] is inadequate since it leads to a gross error. Thus, an alternative approach to extract the capacitance and permittivity can be used considering the electrical response in a high frequency range (10^5–10^7 Hz) using equation (3):

$$-\mathrm{Im}(Z) = 1/\mathrm{j}C_b 2\pi f \tag{3}$$

where $-\mathrm{Im}(Z)$ is the opposite of the imaginary part of the impedance (Z), j is the operator $\sqrt{-1}$ and ω is the angular frequency ($\omega = 2\pi f$).

Considering equation (3), the capacitance of the sample, C_b, is given by the slope of the straight line determined by the variation of $-\mathrm{Im}(Z)$ as a function of $1/2\pi f$. Since the capacitance (C_b) was determined, the permittivity, ε, can be calculated based on equation (4):

$$\varepsilon = C_b l/(\varepsilon_0 A) \tag{4}$$

where ε_0 is the vacuum permittivity, l the thickness of the sample and A the electrode area.

As an example, figure 1(a) represents the impedance diagram obtained at 400 °C in dry air for the $Na_{0.85}Li_{0.15}NbO_3$ sample. The evolution of $-\mathrm{Im}(Z)$ as a function of $1/\omega$ is linear between 10^5 and 10^7 Hz (figure 1(b)).

Applying this relation implies that the response of the imaginary part of the impedance is purely capacitive. This determination can, therefore, be made unambiguously. Moreover, this calculation allows for permittivity values to be reached in a wide temperature range. In this study, the permittivity as a function of temperature was evaluated from 25 to 750 °C.

Figure 2 shows the permittivity values of the $Na_{0.85}Li_{0.15}NbO_3$ system as a function of the temperature for the first thermal cycle (heating and cooling). Two different maxima in the permittivity curve were clearly identified in the temperature range studied. The first maximum, large and well defined, was observed at around 250 °C. The second, higher intensity maximum

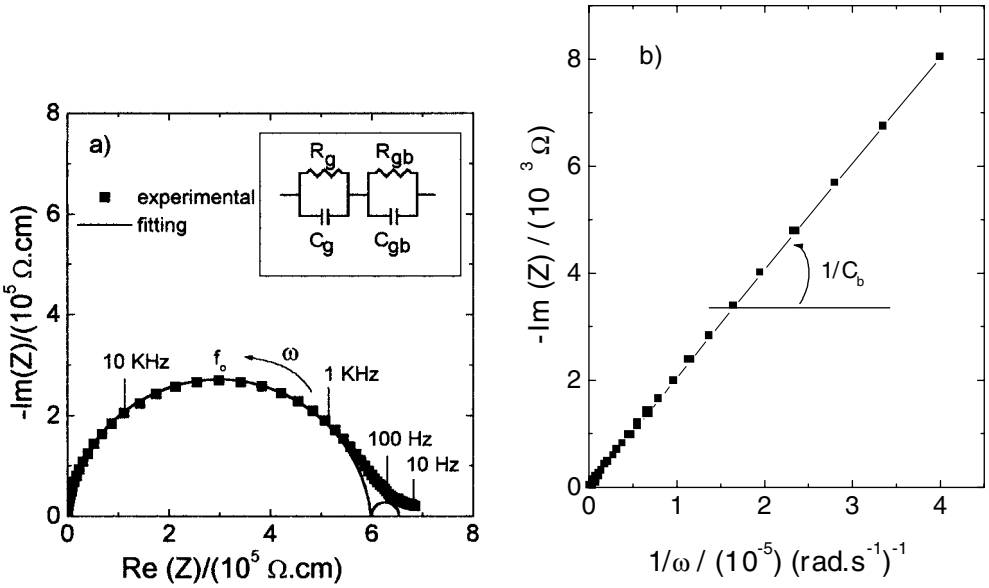

Figure 1. (a) Impedance diagrams of polycrystalline $Na_{0.85}Li_{0.15}NbO_3$ at 600 °C. Two parallel *RC* equivalent circuits are shown in the inset, corresponding to the electric and dielectric response of the solid solution. (b) Evolution of $-\mathrm{Im}(Z)$ as a function of $1/\omega$ of $Na_{0.85}Li_{0.15}NbO_3$ at 600 °C, in the frequency range of 10^5–10^7 Hz.

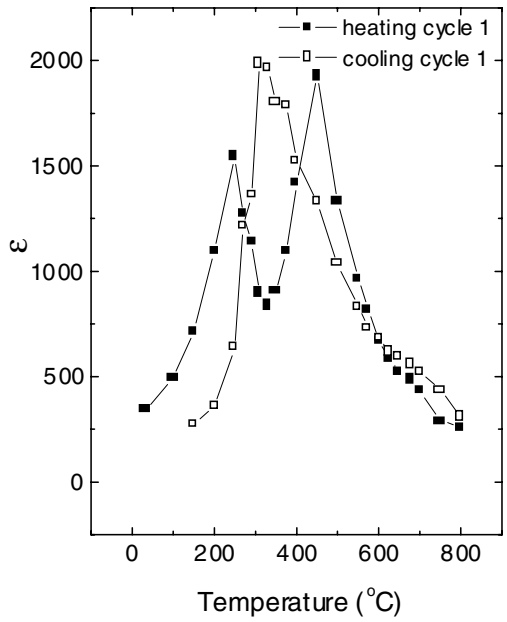

Figure 2. Permittivity as a function of temperature for the first thermal cycle.

was found at 400 °C while a third one, with low intensity, in the form of a shoulder, was identified at around 600 °C.

The presence of maxima in the curves of the permittivity as a function of the temperature in $Na_{1-x}Li_xNbO_3$ has been ascribed to phase transitions [13–16].

During cooling, a decrease was identified in the temperature range between the two peaks with similar intensities at around 300 °C and 350 °C. However, the curves obtained during cooling displayed a different behaviour from that obtained during heating. The two peaks described earlier, between 250 °C and 400 °C, were not observed here. A decrease in the thermal range between the transitions showed a tendency for the two peaks to disappear, resulting in the formation of a large single peak in this interval. However, the shift of the peak position between heating and cooling showed a partial overlapping of the temperature range for the phase transitions. The permittivity, in particular its peak position and intensity, were clearly dependent on the thermal cycle.

An investigation of the partial phase diagram of polycrystalline $Na_{1-x}Li_xNbO_3$, in the composition range of $0.015 \leqslant x \leqslant 0.15$ [3, 14], showed the presence of two phase transitions: orthorhombic–tetragonal at around 200 °C and tetragonal–cubic at about 400 °C, which was associated with the Curie temperature. According to these studies, the temperature at which these phase transitions occurs is a function of the composition, evolving to regions of lower temperature with increased concentrations of lithium. It has been reported that, in the $Na_{0.98}Li_{0.02}NbO_3$ single crystal, the orthorhombic–tetragonal phase transition occurs at around 250 °C. In this system, experiments at temperatures above 360 °C have shown the formation of new domains parallel to the [101] direction, which were associated with a change of crystallographic orientation from 500 °C [7]. These domains tend to disappear at around 660 °C with the formation of the cubic phase. This temperature is known as the ferroelastic Curie temperature.

In this paper, the three phase transitions identified in a higher temperature range were ascribed to orthorhombic–tetragonal, tetragonal–cubic distorted and cubic distorted–cubic phases [7], according to the above described investigation. Based on the behaviour observed in the ε–T curve during cooling, it is reasonable to propose that a symmetry structure mixture is present in the overlapped region. In the $Na_{0.85}Li_{0.15}NbO_3$ system, a thermal hysteresis was observed in each thermal cycle studied.

Moreover, the increased number of cycles led to a decrease of the thermal hysteresis. This variation occurred due to the decrease and shift of the permittivity values around the transition temperatures.

Zhang *et al* [17] have suggested that thermal hysteresis in $Na_{1-x}Li_xNbO_3$ systems is related to the coexistence of the phases, according to a first-order phase transition. Another interpretation is that hysteresis originates in the phase transition process, based on the major structural changes to which the $Na_{1-x}Li_xNbO_3$ system is subjected [17]. An accurate analysis of the position of the peaks and of the phase transitions in the ε curves was made using an innovative approach. The procedure consists of deconvoluting the total polarization of the permittivity response [18].

Figure 3 illustrates the deconvolution of the ε–T curves. The Gaussian function, which provided a good fitting curve, was used in this procedure.

Figures 3(a) and 3(b) show, as an example, the deconvolution of the ε–T curve obtained for $Na_{0.85}Li_{0.15}NbO_3$ in the first thermal cycle (heating and cooling). The straight line results from the combination of the dotted lines, indicating good agreement with the experimental data.

Table 1 summarizes the temperatures extracted from the ε–T deconvolution curves in three thermal cycles. As shown by the results in table 1, the peak positions displayed a tendency to shift to a high temperature during the heating cycles and shift to a low temperature during the cooling cycles. These differences between phase transition temperatures indicated that

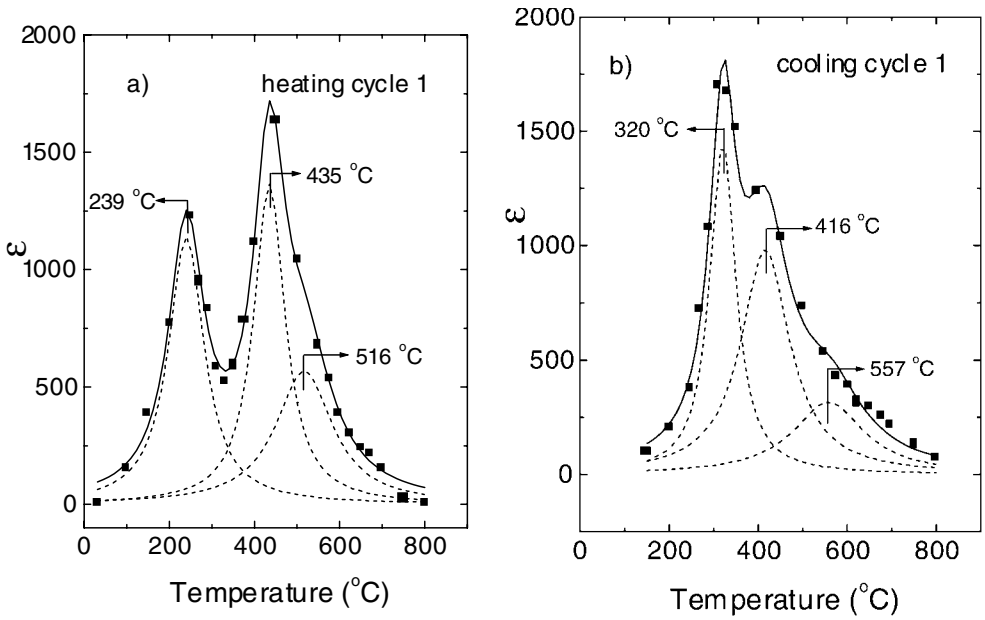

Figure 3. Measured (square points) and fitted (solid line) permittivity as a function of the temperature curve during: (a) heating and (b) cooling in the first thermal cycle. The fitting for individual permittivity contributions (dotted line) is also shown.

Table 1. Phase transition temperatures extracted for the fitted permittivity curves for several cycles in the heating and cooling steps, respectively.

	Temperature (°C)—(heating)			Temperature (°C)—(cooling)		
Cycles	Peak 1	Peak 2	Peak 3	Peak 1	Peak 2	Peak 3
First	239	435	516	320	416	557
Second	302	392	532	297	352	506
Third	306	397	541	—	—	—

ε–T curves were apparent responses. The approximation of the first and second maximum in the permittivity curve, characterized by orthorhombic–tetragonal and tetragonal–cubic phase transitions, showed that the increasing number of cycles caused the character of the transitions to become increasingly diffuse. Naturally, this diffuse behaviour maintained a direct correlation with the phase transition process. Indeed, the phases displaying distinct symmetries at approximately the temperature of phase transition can be considered characteristic of $NaNbO_3$ [19, 20]. A higher degree of overlapping of the characteristic temperature range of each phase transition occurred during the cooling cycles than that developed during the heating cycles. Thus, more complex curve shapes than those obtained in the heating cycles were generated.

Figure 4 shows the loss tangent ($\tan\delta$) derived for 1 kHz in three heating steps. A slope change is located close to 658 °C, suggesting the presence of a phase transition in this region. A slope change at 640 °C was observed in the Arrhenius diagram of $Na_{0.85}Li_{0.15}NbO_3$ [21], thus providing additional evidence of phase development at around 658 °C. Based on the above assumption, a phase transition in the range of 600 to 660 °C can be considered. It is compatible with the very slight permittivity response observed in figures 2, 3(a), 3(b) and 5. According to

Sadel *et al* [7], an isotropic structure (pseudo-cubic) is reached for temperatures above 640 °C in $Na_{1-x}Li_xNbO_3$ systems. This investigation was carried out in the $Na_{0.98}Li_{0.02}NbO_3$ single crystal and was reported as a ferroelastic prototype transition [5, 7]. The inset in figure 4 shows a linear dependence of loss tangent on temperature in the 300 to 400 °C range. This region corresponds to the phase transition region, which involves transitions from higher to lower symmetries. However, no change of phases was observed in this curve and range.

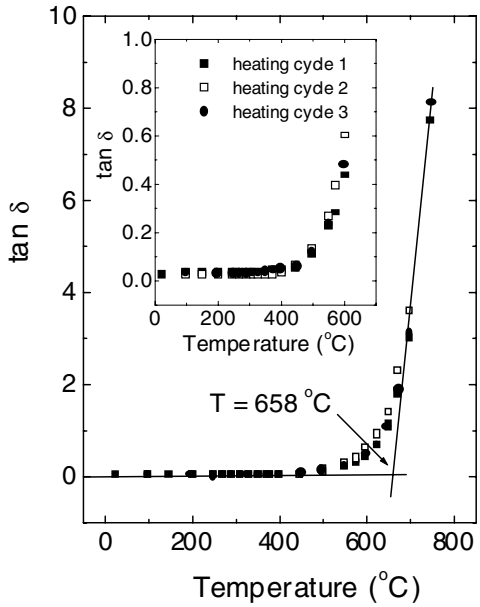

Figure 4. Loss tangent variation (at 1 kHz) of $Na_{0.85}Li_{0.15}NbO_3$ in three thermal cycles.

After analysing the above results, the $Na_{0.85}Li_{0.15}NbO_3$ sample was subjected to a second 2 min thermal treatment at the same sintering temperature.

Figure 5 shows a similar dielectric behaviour as that observed in the first heating cycle (figure 2). Therefore, the variations introduced by the three thermal cycles (table 1) were eliminated in the second thermal treatment at the sintering temperature. Despite the phase transition temperature changing with cycle, the hysteresis area only changes slightly as a function of temperature for the second and third cycles. In fact, large hysteresis is only observed for the first cycle.

The reestablishment of the dielectric characteristics revealed the existence of a phase memory effect in the system. The sintering temperature allows the necessary structural mobility to achieve a metastable configuration. Additionally, experimental evidence suggested that, in terms of the coexistence of distinct symmetry structures, the system was in a state of metastable equilibrium.

4. Conclusion

The permittivity of the $Na_{0.85}Li_{0.15}NbO_3$ polycrystal depends on the presence of the phase with different symmetry structure. The general symmetry is a function of a partial or a complete thermal cycle. The $Na_{0.85}Li_{0.15}NbO_3$ polycrystal phase undergoes four phase transitions from room temperature to 750 °C. Each phase transition temperature can be changed over a wide

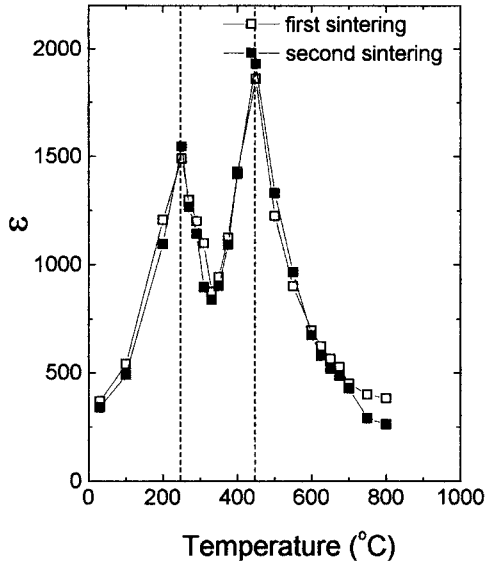

Figure 5. Permittivity as a function of the temperature for the second thermal treatment, at the same temperature as the sintering.

range, depending on the sample's thermal history. The existence of a reversible character for overall phase symmetries determines a phase memory effect.

Acknowledgments

This work was supported by the Brazilian research funding institutions CAPES and FAPESP under contracts Nos 97/04760-5, 98/00758-9 and 99/03749-3. The authors wish to acknowledge Companhia Brasileira de Metalurgia e Mineração—CBMM-Araxá-MG for its supply of niobium complex salt.

References

[1] Zeyfang R R, Henson R M and Maier W J 1977 *J. Appl. Phys.* **48** 3014
[2] Sadel A, Von der Mühll R, Ravez J and Hagenmuller P 1983 *Ferroelectrics* **47** 169
[3] Henson R M, Zeyfang R R and Kiehl K V 1977 *J. Am. Ceram. Soc.* **60** 15
[4] Megaw H D 1974 *Ferroelectrics* **7** 87
[5] Sadel A, Von Der Mühll R, Ravez J, Chaminade J P and Hagenmuller P 1982 *Solid State Commun.* **44** 345
[6] Von Der Mühll R, Sadel A and Hagenmuller P 1984 *J. Solid State Chem.* **51** 176
[7] Sadel A, Von Der Mühll R and Ravez J 1983 *Mater. Res. Bull.* **18** 45
[8] Lanfredi S and Rodrigues A C M 1999 *J. Appl. Phys.* **86** 2215
[9] Lanfredi S, Folgueras-Domínguez S and Rodrigues A C M 1995 *J. Mater. Chem.* **5** 1957
[10] Lanfredi S, Dessemond L and Rodrigues A C M, 2000 *J. Eur. Ceram. Soc.* **20** 983
[11] Bauerle J E 1969 *J. Phys. Chem. Solids* **30** 2657
[12] Cole K S and Cole R H 1941 *J. Chem. Phys.* **9** 341
[13] Von Der Mühll R, Sadel A, Ravez J and Hagenmuller P 1979 *Solid State Commun.* **31** 151
[14] Nitta T 1968 *J. Am. Ceram. Soc.* **51** 626
[15] Cross L E and Nicholson B T 1955 *Phil. Mag.* **46** 453
[16] Shirane G, Newnham R and Pepinsky R 1954 *Phys. Rev.* B **96** 581
[17] Zhang P L, Zhong W L, Zhao H S, Chen H C, Chen F S and Song Y Y 1988 *Solid State Commun.* **67** 1215
[18] Chen Z-Y, Katiyar R S, Yao X and Bhalla A S 1998 *Phys. Rev.* B **57** 8166

[19] Kus C, Ptak W S and Smiga W 1991 *Ferroelectrics* **124** 249
[20] Badurski M, Handerek J, Szatanek J and Szot K 1979 *Acta Phys. Pol.* A **55** 835
[21] Nobre M A L and Lanfredi S 2000 *J. Mater. Chem.* submitted